

Optimizing the removal of iron oxide from Egyptian feldspar ore

Khaled E. Yassin, A.M. Elbendari, El-Sayed R. E. Hassan

Minerals Beneficiation and Agglomeration Department, Minerals Technology Division, Central Metallurgical Research & Development Institute (CMRDI), P.O. Box 87 Helwan, 11722 Cairo, Egypt

Corresponding author: prof_s_elsaidy@yahoo.com (El-Sayed R. E. Hassan)

Abstract: The demand for feldspar as a raw material for various industrial applications continuously increases. Feldspar is a primary raw material in manufacturing ceramics, glass, fillers, welding electrodes, and enamel. Feldspar is often associated with iron oxide, which decreases its economic value and hinders its industrial application. The present work aimed at reducing iron oxide content in Egyptian feldspar ore from the Wadi Zerabi locality. Ball milling was used for preparing feldspar feed of size -250+45 μ m. CarpcO dry high-intensity magnetic separation followed by acid leaching processes were carried out in order to decrease the iron contamination and increase the feldspar content. A Box-Behnken statistical design was used to optimize the magnetic separation results. From a feldspar feed containing 1.40% Fe₂O₃, a non-magnetic concentrate of 0.25% Fe₂O₃ was obtained. The Fe₂O₃ removal reached up to 82% with a high yield as the % weight of non-magnetic feldspar reached up to 97.5%. The leaching process further reduced the iron oxide content down to 0.19 %. Also, the feldspar whiteness was improved from 65.17% in the original ore to 85.60% in the leached product.

Keywords: feldspar ore, iron oxide contamination, ball mill, CarpcO magnetic separator, acid leaching, whiteness

1. Introduction

Feldspar is one of the most common minerals in the world, and it forms about 60% of the rocks in the Earth's crust (Pane et al., 2022). The most widespread feldspar minerals are orthoclase (K-feldspar), albite (Na-feldspar) and anorthite (Ca-feldspar). The most associated minerals in feldspar ore are clays, mica, rutile, and silicates (Amareih and Al-Jardin, 2014). Depending on the types of minerals and their particle sizes, raw materials are processed using various mineral processing techniques to remove impurities. Magnetic separation is the most common method for eliminating iron-bearing minerals, the primary coloring impurities that adversely affect product quality. Iron and titanium minerals have existed in the mineralogical structures of feldspar. They are known as unwanted impurities because of their coloring properties. Therefore, Fe₂O₃ and TiO₂ contents of 0.30% or below are required in feldspar to meet the demands of ceramic and glass industries (Zhang et al., 2018). For example, in ceramic production, iron and titanium-bearing minerals harm the color of the product (Cinar and Durgut, 2019; Ibrahim et al., 2002; Pane et al., 2022). Due to the magnetic properties of iron minerals, mica, and garnet in feldspar ore, it can be separated from feldspar minerals by the external magnetic field.

The gangue minerals in feldspar generally appear to have weak magnetic properties; therefore, using a high-intensity magnetic separator could produce a good-quality final product. Magnetic methods are applied to nepheline syenite about the mineral type and particle liberation size (Abouzeid and Negm, 2014; Ahmed et al., 2016; Jena et al., 2014). The dry magnetic separation method separates magnetic minerals from feldspar ore for use primarily in ceramic bodies (Jena et al., 2014). It can also be used for pre-enrichment because it works best with particles of a higher size range. The grade of the concentrate that is made after dry magnetic separation can be raised even more by using wet magnetic and flotation methods, which free up more mineral particles (Gougazeh, 2006; El-Rehiem and Abdel-Rahman, 2008). As a result, efficient separation of Fe-bearing minerals on a commercial scale and in an environmentally benign manner could be achieved (Saisinchai et al., 2015). A Turkish feldspar sample was processed in

a rare earth roll magnetic separation to separate the colouring impurities (Gülsoy et al. 2004, Gülsoy et al. 2005). They came to the conclusion that a suitable size fraction should be fed to a specific magnetic separator or the magnetic separator should be designed specifically for the material that is to be concentrated. A high-grade potassium feldspar concentrate composed of 0.11% Fe₂O₃, and 0.04% TiO₂ was produced.

Liu et al. (2013) used high intensity wet permanent magnetic separator (HIWPMS) system to substitute the high intensity electromagnetic separators of fine feldspar ore (85 % less than 75 micron). Feldspar product containing 0.17% Fe was obtained from a feed having 1.31% Fe. Saisinchai et al. (2015) employed wet high intensity magnetic separation (WHIMS) as a replacement for the reverse flotation of magnetite and rutile, yielding a feldspar product with a composition of 68.29% SiO₂, 18.69% Al₂O₃, 0.07% Fe₂O₃, 5.83% K₂O, and 6.33% Na₂O. This approach enabled the effective separation of iron-bearing minerals on a commercial scale in an environmentally being manner could be achieved.

Moreover, Xu et al. (2022) developed a novel dry vibrating high-gradient magnetic separator (DVHGMS) for eliminating iron ores from potash feldspar. The vibration dispersed feldspar particles and improved the separation efficiency thus, the Fe₂O₃ content was reduced from 0.191% to 0.035% with feldspar mass weight of 92.35%. Also, Gougazeh (2022) studied the beneficiation of low-grade Saudi Arabia feldspar ore using a combination of dry high-intensity magnetic separation and direct cationic flotation under 500 g/ton dosage of Aero 801 + Aero 825 + Aero 830 mixture at pH 3. A feldspar concentrate of 65.18% SiO₂, 0.06 wt.% Fe₂O₃ and 0.09 wt.% TiO₂ was obtained.

Because of the low cost of processing, acid leaching for removing Fe from feldspar ores after magnetic separation is an alternative way. Organic acids which have -COOH groups in their chemical formula, are less corrosive than inorganic ones, can be used to dissolve iron impurities. Moreover, they are biodegradable and can achieve a higher metal extraction efficiency at mildly acidic pH compared to other extracting agents (Jonglertjunya and Rubcumintara, 2013; Del Dacera and Babel, 2006; Cameselle et al., 2003). So, feldspar is leached by organic acids and biological methods which replaced mineral acids ((Abouzeid and Negm, 2014; Iveta et al., 2005). In the same time agglomeration or selective flocculation methods are also used for enrichment of feldspar (Dogu, 2004).

Most studies on iron removal from clays focus on kaolin (Kar et al., 2013; Abdel-Khalek et al., 2019), with fewer investigations conducted on feldspars (Zhang et al., 2018). Styriakova et al. (2003) explored feldspar treatment using heterotrophic bacteria, achieving a 31% iron dissolution after 120 days, with accelerated dissolution through the addition of 0.1 M oxalic acid. Arslan et al. (2008) examined optimal conditions for oxalic acid leaching, employing a two-stage leaching process and achieving 72.59% iron removal from feldspar at the optimum condition (5% solids, 0.2 M oxalic acid concentration, temperature of 80°C, and 120 min reaction time). Vapur et al. (2017) investigated iron removal using organic acids, with oxalic acid achieving Fe% and Ti% removal of 80.44% and 45.39% respectively under optimal conditions (4% solid/liquid ratio, 1.1 mol/dm³ oxalic acid concentration, 88 °C and 48 min). Pariyan et al. (2020) studied iron dissolution from Iranian feldspar using oxalic acid, employing initial tests to determine optimal parameters. Through central composite experimental design, they achieved an 85% iron removal under conditions of 70°C, 1000 rpm, 5% S/L ratio, 20 g/l oxalic acid, and 90 minutes. The kinetics of iron dissolution exhibited a reasonable fit with the shrinking core model with a mixed control mechanism.

The present study aims at removing iron oxide from Egyptian feldspar to get a feldspar product with specifications suitable for different industrial application. For that, the feldspar sample will be ground using ball mill to prepare a feed of -250+45µm suitable for the upgrading processes. Then, optimizing the Carpc magnetic separator's parameters for better feldspar upgrading. A Statistical experimental design methodology will be applied for better separation of the iron-bearing contaminants. Also, a study on leaching of the non-magnetic feldspar will be introduced to enhance feldspar whiteness.

2. Materials and methods

A low-grade Egyptian feldspar sample from the Wadi Zerabi region of the Eastern Desert was used for this study. Oxalic and citric acids were purchased from El-Nasr for Chemical Industries Co. (Egypt). All solutions were freshly made at room temperature shortly before using. Bi-distilled water was used to prepare all the solutions.

2.1. Feldspar ore preparation

The feldspar sample was, first, primary crushed in a “5x6 Denver” Jaw crusher followed by secondary crushing using a “Wedag” roller to produce a product of size less than 2 mm. The crushed products were wet ground using a laboratory ball mill having the dimensions of $D \times L = 150 \times 200$ mm and screened in 250 and 45 μm sieves to determine the percentage of +250 μm , -250+45 μm and -45 μm size fractions. The experiments were performed at a constant speed of $n = 76$ rpm which is 70% of its critical speed. The mill charge consisted of forged steel balls with density $\rho_b = 7.8$ g/cm³, Table 1. The milling was carried out until the entire sample passed from 250 μm .

Table 1. Wet ball mill grinding test conditions

Item	Description	
Mill	Inner diameter (D), mm	150
	Length, mm	200
	Volume, cm ³	3532
	Mill speed Critical (N_c) ^a [rpm]	109
	Operational speed, Φ_c (0.7)	76
Media (Balls)	Material	Forged steel
	Specific gravity	7.8
	Mass of balls, g	4150
	Assumed porosity	40 %
	Ball size	36.6
	Ball filling volume fraction (J) ^b , [%]	25
Material	Feldspar ore	
	Specific gravity, g/cm ³	2.6
	Initial feed size	2ml
	Powder filling (f_c) ^c , [%]	5
	% S in slurry by weight	65%
	Interstitial filling (U) ^d , [%]	0.5

where Eqs. (1-4) (Zhao et al., 2017 and Magdalinovic et al., 2012):

$${}^a N_c = \frac{42.3}{\sqrt{D-d}} \quad (1)$$

$${}^b J = \left(\frac{\text{Volume of solid balls}}{\text{Mill volume}} \right) \times \frac{1}{0.6} \quad (2)$$

$${}^c f_c = \left(\frac{\text{Volume of powder}}{\text{Mill volume}} \right) \times \frac{1}{0.6} \quad (3)$$

$${}^d U = \frac{f_c}{0.4 J} \quad (4)$$

2.2. Feldspar characterization

2.2.1. Chemical analysis

Quantitative chemical analysis of the oxide content in original and produced feldspar samples was conducted using X-ray fluorescence spectrophotometer (XRF), Model (WD axios advanced) Panalytical, Netherlands, The AXIOS uses SuperQ software for standard-based analysis. It is used for detecting the major oxides and trace elements present in the feldspar sample. A 10g of the sample is mixed and pressed with 2gm of wax as a binder in aluminum cup, and then exposed to X-ray as a disk. The instrument is connected to a computer unit with software program to calculate the elements as oxide forms. The limit of detection in the WD-XRF method for Fe is approximately 0.03 % with estimated error of $\pm 0.004\%$.

2.2.2. XRD analysis

Qualitative X-ray diffraction (XRD) analysis was conducted to determine the phase composition of the minerals. It was performed using PAN analytical X'Pert PRO with Secondary Monochromator, Cu-

radiation ($\lambda=1.542\text{\AA}$) at 45 K.V., 35 M.A., and scanning speed $0.04^\circ/\text{sec}$. were used. The diffraction peaks between $2\theta=2^\circ$ and 80° , corresponding spacing ($d, \text{\AA}$), and relative intensities (I/I_0) were obtained. The diffraction charts and relative intensities are obtained. Feldspar samples are submitted as a fine powder, -75 micron, and placed on the sample stage. The intensities of the pattern peak are determined by the atoms distribution within the lattice. The x-ray diffraction pattern is specific to the periodic atomic arrangements in a given material, which is compared to the ICDD standard database of x-ray diffraction patterns for phase identification.

2.2.3. Thin section preparation

Feldspar specimens were ground as the surfaces are parallel to each other. One side of the ground surfaces is then carefully polished on a glass plate, and glued on a slide glass with Canada balsam as the polished surface is faced to the glass plate. The glued specimen is polished until it becomes 0.03 mm thick, and then, it is covered with a slide glass.

2.2.4. Optical properties

"UV whiteness and color-meter model JY 98" was used to measure the non-magnetic fraction's whiteness following magnetic separation and leaching. The whiteness, brightness, iso-brightness, redness and yellowness % were measured for original and treated feldspar samples. The sample was put in the dryer for two hours at 100°C to be completely dry. About 10g of dried sample was compressed by a powder mold. The smooth surface of compressed sample exposed to UV lamp in the measuring port. The equipment is connected to the computer and printer for outputting the results.

2.2.5. Magnetic susceptibility

The Magnetic susceptibility of original and treated feldspar samples was measured using a susceptibility meter "Bartington, UK" MS3 sensor and an MS2G meter assembly for powder samples connected to a computer for data display and saving. The samples were placed in 1-cm^3 plastic vials for measurement after calibration using a calibration sample provided by the manufacturer. The MS2G meter has a field amplitude of $500\ \mu\text{T}$ and a 1.3 kHz operating frequency. Three measurements were carried out, and the average is reported in this paper. The output results are dimensionless and measured using the cgs system (Elmahdy et al., 2023).

2.3. Feldspar upgrading:

2.3.1. Magnetic separation

The ground feldspar samples of $(-250+45\ \mu\text{m})$, was supplied to the laboratory Carpco dry high intensity magnetic separator (Lift-Type Induced Roll, Model MLH-13-111-5). Its processing capacity of granular material up to $1.5 \times 10^3\ \text{g}/\text{min}$, variable magnetic field intensity of up to 0.95 tesla, and 127mm diameter \times 50.8mm length laminated roll with a changeable speed 5-300 rpm (Ibrahim et al., 2002). It is intended to separate components that are moderately or weakly magnetic (para-magnetic) from non-magnetic components. A dry feed of -250+45 micron is fed via a top-feeder. The feed material is passed through the magnetic field, and the magnetic iron oxide particles are attached to the roll and separated from the nonmagnetic feldspar stream. Three parameters could be studied which are feed rate (g/min), roll speed (rpm) and field intensity (tesla) (Hassan et al., 2020).

2.3.2. Leaching process

For the purpose of improving the quality of the concentrate produced at the optimum conditions of the magnetic separation process, the concentrate was leached using oxalic and citric acids to dissolve iron oxide. Leaching tests were conducted with a magnetic stirring-hot plate in a beaker ($250\ \text{cm}^3$), and the temperature was controlled by a thermometer. A 10 g sample was heated for 60 min. at 90°C as optimized previously by Abdel-Khalek et al., (2019) and the leaching process was carried out at a S/L ratio of 5% with continuous stirring speed of 1000 rpm (Pariyan et al. 2020). The effect of acid type, using oxalic and citric acids, with acid dosage ranged from 1.0 to 4.0 kg of organic acid per ton of the non-

magnetic feldspar fraction. on $\text{Fe}_2\text{O}_3\%$ and its % removal were investigated. At the end of the test, the slurry was filtered and dried in a dryer at 80°C . Then, the products were chemically analyzed.

3. Results and discussion

3.1. Mineralogy and chemical composition of the sample

Table 2, shows XRF analysis of the sample, the sample contains: 75.85% SiO_2 , 12.48 % Al_2O_3 , 1.40% Fe_2O_3 , 3.22% Na_2O , 5.36% K_2O , and 0.93% CaO . From these results the sample belong to K-feldspar

Table 2. XRF of Wadi Zerabi feldspar ore sample

Oxide	SiO_2	Al_2O_3	Na_2O	K_2O	Fe_2O_3	TiO_2	CaO	MgO	Cl	L.O.I
%	75.870	12.480	3.220	5.360	1.400	0.091	0.930	0.074	0.040	0.533

Fig. 1 shows XRD of the original feldspar sample. It contains albite and microcline as the main feldspar minerals while quartz is the main gangue with minor amount of hematite impurities. These results were confirmed by mineralogical studies.

According to the petrographic analysis, the rock has the name altered leucocratic granite and is a plutonic, acidic igneous rock. It has granular, muscovite, and chlorite well-developed perthitic (intergrowth of plagioclase and alkali feldspar), micrographic, and poikilitic textures and is medium to quite coarse-grained. Some micro-fractures are observed cutting through the rock, as shown in Fig. 2, (A-E). Opaque minerals present in rare amounts that occur as very fine to fine-grained, irregular disseminations in the rock.

Fig. 2 (A-E) displays the existing minerals in the feldspar ore sample through the thin section under the microscope with zoom (25X, C.N.). Potash feldspar, quartz, and plagioclase constitute the majority of feldspar, with minor amounts of hematite and muscovite minerals. Potash feldspar and soda feldspar are represented by microcline and albite minerals, which occur as coarse to medium-grained anhedral crystals that are partially altered to clay. One of the most essential substances in minerals is quartz. It appears as anhedral, medium to coarse crystals, including intergrowth with potash feldspar and soda feldspar, and has a graphic texture.

Photomicrographs showing all minerals in the Wadi Zerabi feldspar sample through the thin section; A) Perthite and granophyric texture in head sample, B) Plagioclase, Quartz and Microcline, C) Plagioclase and Quartz as major, minerals, D) Micro veinlet of Quartz, perthite and microcline, E) Hematite and Muscovite (thin section 25X, C.N.).

3.2. The effect of grinding time on crushed feldspar

Grinding is a key step in mineral processing technology for producing necessary particle sizes and liberating valuable minerals from gangue for further concentration (El-Mofty et al., 2020)

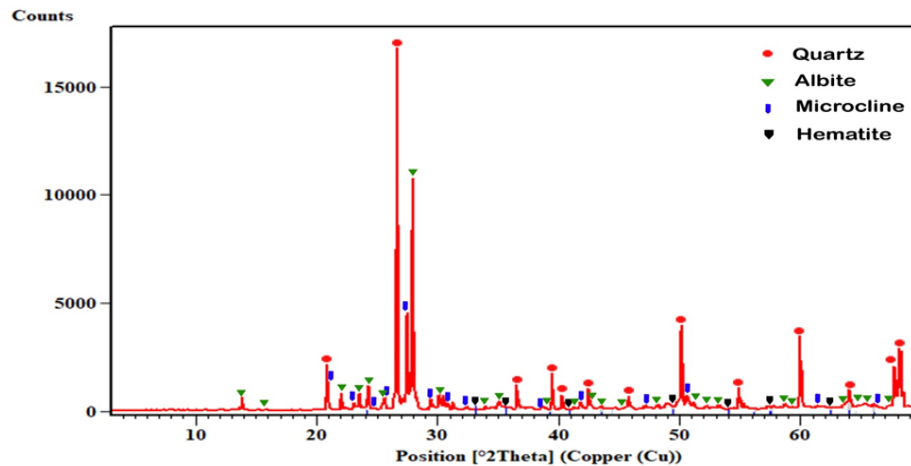


Fig 1. XRD of Wadi Zerabi feldspar sample

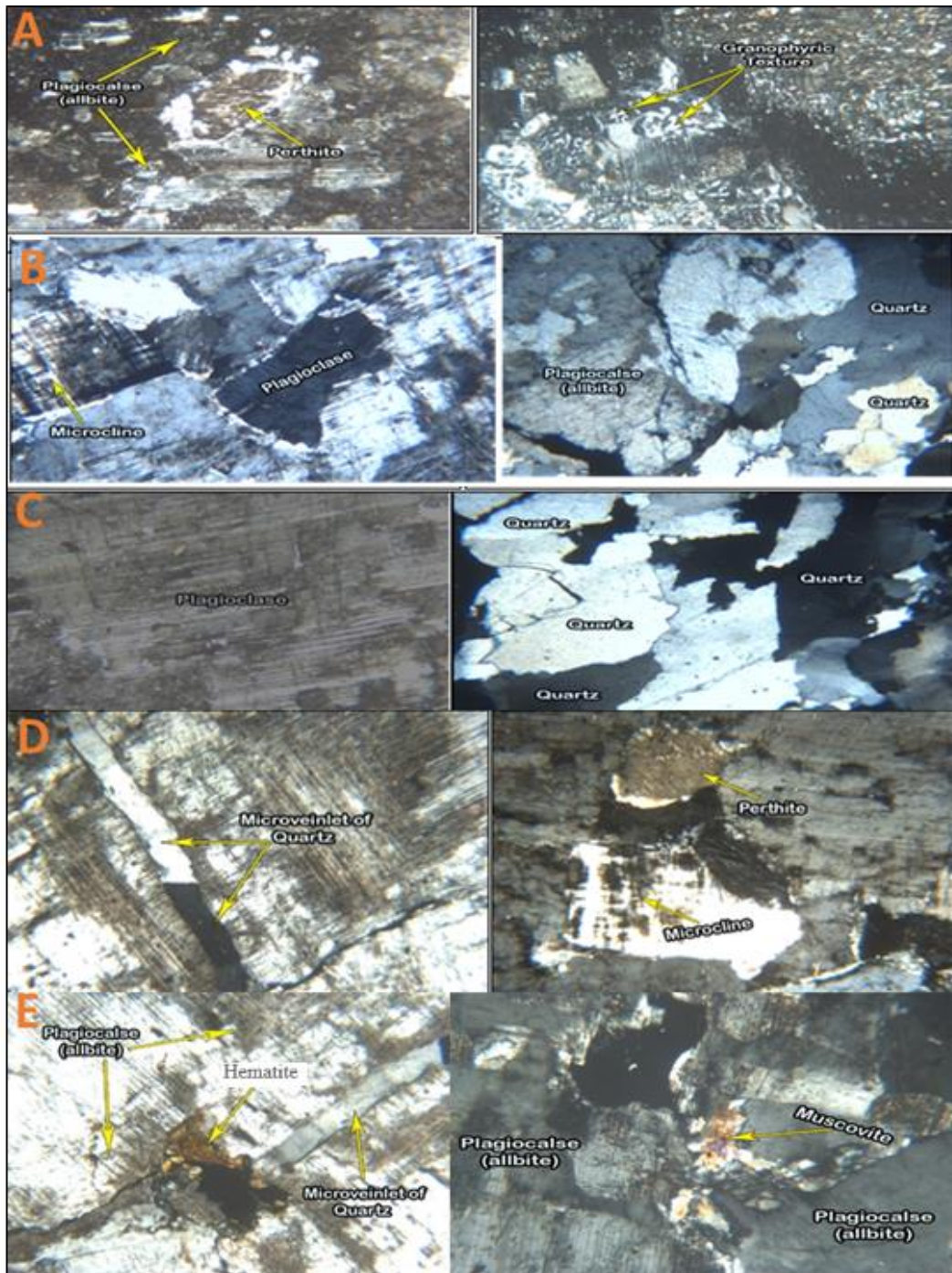


Fig. 2. Photomicrographs showing all minerals in feldspar sample through the thin section (25X, C.N.)

Grinding is the largest energy-consuming operation in mineral processing. Determination of the mineral liberation size is the first and most crucial step to overcoming this challenge, which eliminates over-grinding and, as a result, lowers the cost of grinding (Elbendari et al., 2020).

In order to avoid overgrinding and to control the produced fines, grinding time must be constantly monitored. The previous studies on Egyptian feldspar (Wadi Zirib locality) proved that the suitable size for subsequent separation processes is less than $250\mu\text{m}$ (Ahmed et al., 2016).

The optimal grinding time for feldspar ore was investigated in order to maximize feed size production for further concentration processes (such as flotation and/or magnetic separation) while minimizing slimes (fine particles less than $45\mu\text{m}$), which negatively affect separation performance. The size distribution of the feed material as defined from dry sieving is presented in Fig. 3. Before grinding, the fraction less than $250\mu\text{m}$ was first separated from the feed. Milling was carried out in fractions of

sizes over $250\mu\text{m}$ at 65% solid content in slurry, 5% powder filling, and 25% ball filling of size 36.6 mm, Table 1. Fig. 4 presents the results of grinding feldspar at different grinding times. The desired size for Carpc magnetic separation ($-250+45\mu\text{m}$) is significantly increased by increasing the grinding time. Further grinding beyond 15 minutes resulted in a reduction in feed size for the magnetic separation process ($-250+45\mu\text{m}$) while maximizing slimes ($-45\mu\text{m}$).

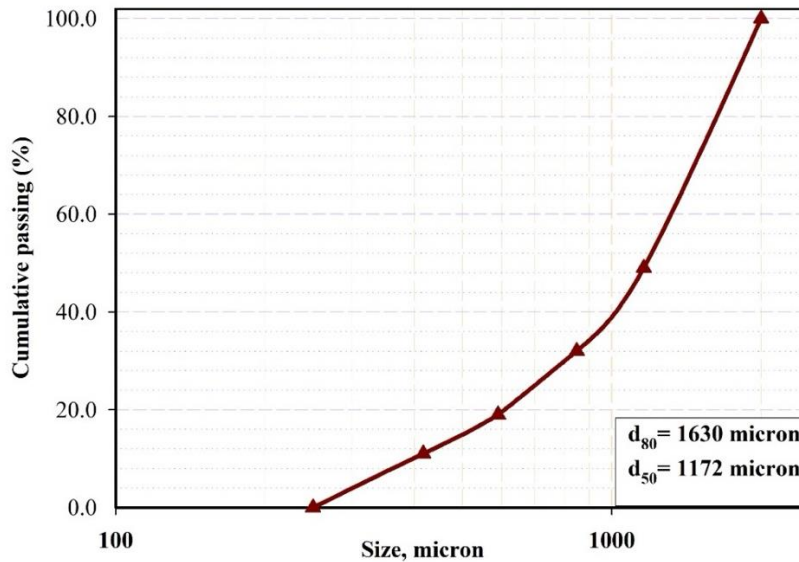


Fig. 3. The particle size distribution of the feldspar feed

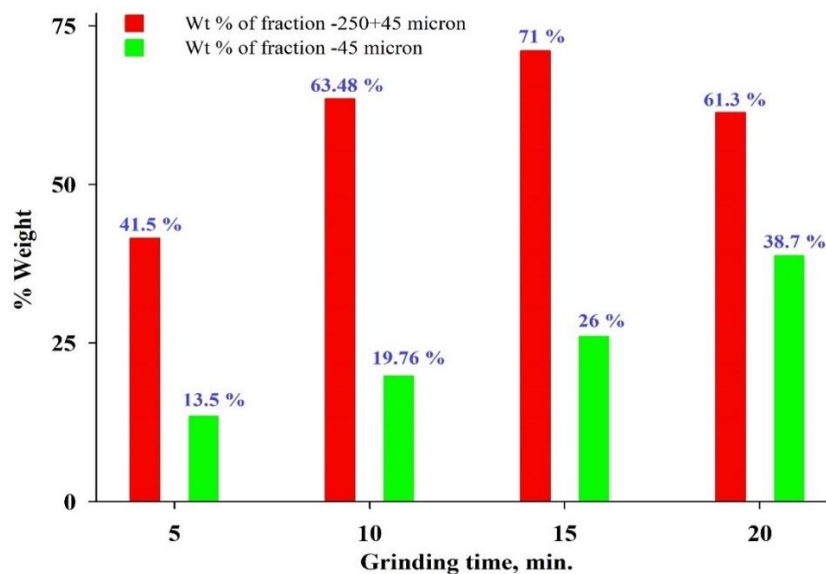


Fig. 4. Effect of grinding time at 65% solid content in slurry, 5% powder filling, and 25 % ball filling of size 36.6 mm

3.3. Parameters affecting on the upgrading of feldspar ore by Carpc magnetic separation

Magnetic separation was carried out in the ground product $-250+45\mu\text{m}$. The fraction less than $45\mu\text{m}$ was stored for further upgrading utilizing other magnetic separation technologies, such as wet high intensity magnetic separation (WHIMS), that are appropriate for fine particles.

The variables investigated in this research are magnetic field intensity, roll speed, and feed rate. These parameters were studied using the classical method, which takes into account one variable at a time while keeping the others constant and identifies the area that has the greatest influence. The statistical design program is then used, which provides details about the interactions of various factors and how the overall system works.

3.3.1. Effect of magnetic field intensity

The magnetic field intensity is one of the most essential variables influencing magnetic separator performance. Fig. 5 shows that with increasing magnetic field, the iron oxide decreased in the non-magnetic fraction, where at magnetic field intensity 0.95 tesla, the iron oxide reduced to 0.30 % from 1.4% in the feed sample, and the percentage of iron removal increased from 30.17 to 79.60 %. The attraction of magnetic particles to the roll increases as the magnetic field intensity increases, and hence, the non-magnetic fraction becomes cleaner as the magnetic field intensity increases (Abouzeid and Negm, 2014; Silva et al., 2019; Ibrahim et al., 2002). The following tests were conducted with a field intensity of 0.95 tesla.

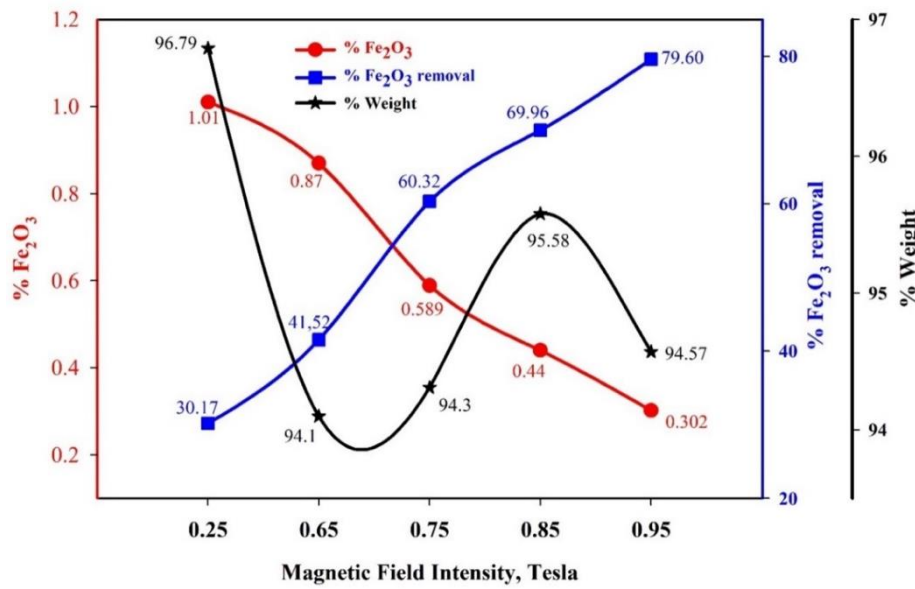


Fig. 5. Effect of magnetic field intensity on iron oxide removal at 120 rpm roll speed, and feeding rate 100g/min

3.3.2 Effect of roll speed

Fig. 6 represents the effect of increasing roll speed on the performance of the magnetic separator. There were five different roll speed settings (30, 60, 90, 120, and 150 rpm), with a constant feed rate of 100g/min. When the roll speed was increased to 120rpm, the iron oxide decreased to 0.30%; however, after 120 rpm, the iron oxide increased in the non-magnetic fraction. This may be related to the fact that increasing roll speed above 120 rpm reduces the probability of particles being attracted to the magnetic roller, resulting in a decrease in separation performance. The roll speed to the separator for the following series was taken as 120 rpm.

3.3.3. Effect of feeding rate

The effect of feed rate on the performance of the magnetic separator is shown in Fig. 7. The iron oxide was reduced from 0.34% at a feeding rate 50 g/min. to 0.257% at a feeding rate 400g/min. after increasing the feeding rate to 600 g/min. the iron oxide increased, according to these results increased till it reached to 82.1% at 400 g/min. then decreased to 81.24% at 600g/min.

Lowering separation performance at higher feed rates of 600g/min may be due to increased ore bed thickness, which hinders the attraction of magnetic particles to the revolving roll (Abouzeid and Negm, 2014; Ibrahim et al., 2002). Based on the obtained results, the most suitable iron oxide separation parameters for the (-250+45 μ m) fraction are 0.95 tesla magnetic field intensity, feeding rate 400 g/min, and 120 rpm roll speed, where iron oxide decreased from 1.4% in the feed to 0.257 %.

3.4. Applying Box-Behnken design

Box-Behnken factorial design was chosen to find out the relationship between the response function (% assay of Fe₂O₃ and its % removal) and three important variables namely; current intensity from 0.75-

0.95 tesla, roll speed from 60-120 rpm, and the feed rate from 100 to 500 g/min. and their influence on Carpc magnetic separation, table 3. The best parameters were estimated according to the design using a second order polynomial function. Using this function, a correlation between studied parameters and response was created. The general form of this equation is (Hassan et al. 2020; Rostom et al. 2020):

$$Y = \beta_0 + \beta_1X_1 + \beta_2X_2 + \beta_3X_3 + \beta_{12}X_1X_2 + \beta_{13}X_1X_3 + \beta_{23}X_2X_3 + \beta_{11}X_1^2 + \beta_{22}X_2^2 + \beta_{33}X_3^2 \quad (5)$$

where Y is the predicted response; % weight of non-magnetic feldspar, % Fe₂O₃ grade and % Fe₂O₃ removal, X₁, X₂ and X₃ are studied variables: magnetic field intensity, roll speed and feed rate; β_{ij} are equation constants and coefficients.

ANOVA data for the feldspar upgrading system implies the well convenience of the experimental results to the polynomial model equation and thus the accuracy of this model, Table 4. The high values of R² indicates that the quadratic equation is capable of representing the system under the given experimental domain. It can be seen that there was a good agreement between predicted and actual values (The Predicted R² is in reasonable agreement with the Adjusted R²); i.e. the difference is less than 0.2. The Adequate Precision ratios proof an adequate signal. The model F-values indicate the model is significant. This model can be used to navigate the design space (Hassan et al., 2020).

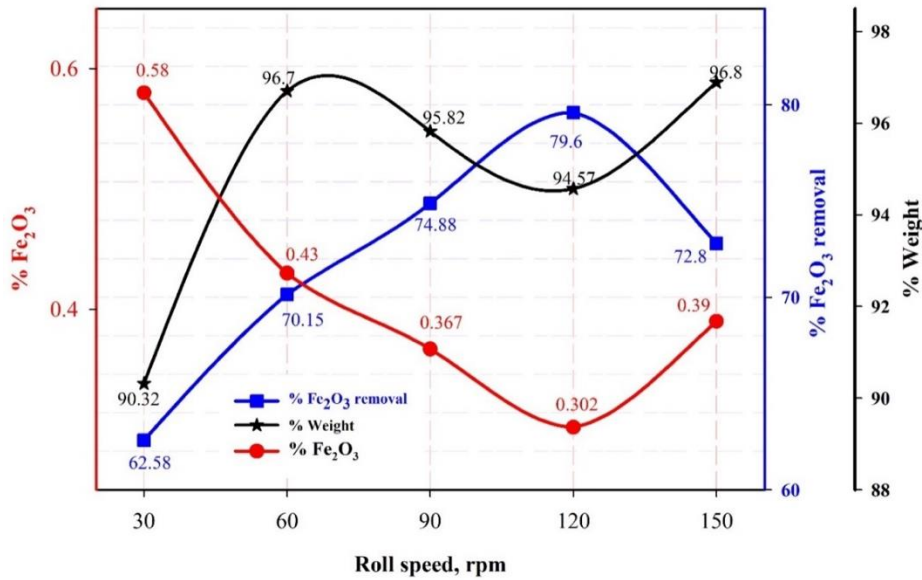


Fig. 6. Effect of roll speed on iron oxide removal at 0.95 T magnetic field intensity and 100 g/min feeding rate

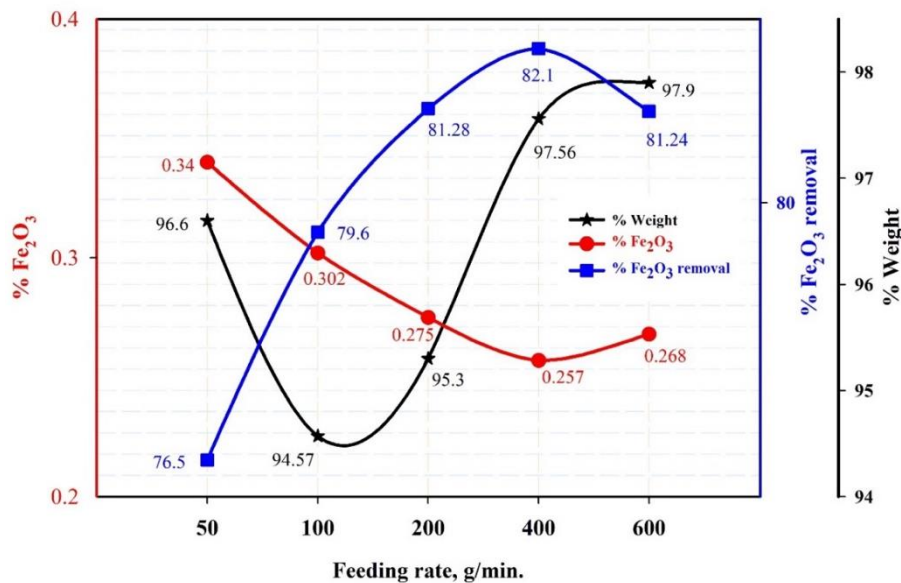


Fig. 7. Effect of feeding rate on iron oxide removal at 0.95 Tesla magnetic field intensity and roll speed 120 rpm

Table 3. Box-Behnken design results for Carpc magnetic separator

Run	Feed rate, g/min	Roll speed, rpm	Magnetic field intensity, tesla	Weight of non-magnetic, %	Fe ₂ O ₃ , %	Fe ₂ O ₃ removal, %
1	100	90	0.75	95.42	0.658	55.43
2	100	90	0.95	96.32	0.365	74.88
3	300	90	0.85	96.39	0.483	66.74
4	300	120	0.75	96.55	0.553	61.86
5	500	90	0.75	96.65	0.593	58.5
6	500	90	0.95	97.11	0.31	79.43
7	100	60	0.85	95.25	0.564	61.64
8	300	60	0.95	96.27	0.403	72.28
9	500	90	0.85	96.85	0.44	69.56
10	500	60	0.85	96.43	0.52	64.96
11	300	60	0.75	95.51	0.683	53.4
12	100	120	0.85	96.45	0.435	70.03
13	300	120	0.95	97.18	0.284	80.29
14	300	90	0.75	96.05	0.618	57.6
15	300	90	0.95	96.72	0.349	75.91
16	500	120	0.95	97.52	0.251	82.51
17	300	90	0.85	96.39	0.483	66.74

Table 4. ANOVA for response surface quadratic model of Carpc magnetic separator

The statistical parameters	Weight % of non-magnetic	Fe ₂ O ₃ , %	Fe ₂ O ₃ removal %
Standard deviation	0.0204	0.0072	0.5699
R-Squared	0.9995	0.9987	0.9982
Adjusted R ²	0.9989	0.9970	0.9960
Predicted R ²	0.9952	0.9900	0.9854
Adequate precision	143.16	80.17	68.1650
F-Values	1601.72	599.64	439.23

The equations in terms of actual factors for the feldspar upgrading system can be used to make predictions about the response for given levels of factors, Weight % of non-magnetic, Fe₂O₃ % and Fe₂O₃ Removal %, in the non-magnetic feldspar concentrate as follows:

$$\text{Weight \% of non-magnetic} = +89.51955 + 0.008462 A + 0.030496 B + 3.82084 C - 0.000014 A * B - 0.005241 A * C - 0.009110 B * C - 3.94633E-07 A^2 - 0.000010 B^2 + 1.18363 C^2 \quad (6)$$

$$\%Fe_2O_3 = +2.28694 - 0.000170 A - 0.002418 B - 2.26469 C - 4.73443E-07 A * B + 0.000150 A * C + 0.001086 B * C - 9.57255E-08 A^2 - 2.90554E-06 B^2 + 0.429331 C^2 \quad (7)$$

$$Fe_2O_3 \text{ Removal \%} = -45.43467 - 0.008345 A + 0.158529 B + 137.14820 C - 0.000012 A * B + 0.014908 A * C - 0.061449 B * C + 9.59126E-06 A^2 + 0.000192 B^2 - 23.75146 C^2 \quad (8)$$

where: A is the feed rate (g/min), B is the roll speed (rpm) and C is the magnetic field intensity (tesla).

Fig. 8 (a,b,c) represents the effects of the studied parameters on the % assay of Fe₂O₃. It has been shown that using Carpc magnetic separator, the most effective parameter influencing on the assay of Fe₂O₃ in feldspar concentrate is the magnetic field intensity.

Fig. 9 (a,b,c) displays the Fe₂O₃ removal % as a function of Carpc separator parameters. It is displayed that the highest magnetic intensity is recommended for efficient removal of Fe₂O₃ from feldspar. Also, high Fe₂O₃ removal from feldspar was obtained at high feed rate and roll speed values. Therefore, increasing the magnetic field intensity from 0.75 to 0.95 tesla decreased Fe₂O₃ assay% while increased both Fe₂O₃ removal % as well as the recovery, weight %, of feldspar in the non-magnetic fraction. It was

shown that there is no great interaction between Carpc variables. Therefore, efficient iron oxide removal from feldspar sample was obtained at the highest studied values of magnetic field intensity, roll speed and feed rate.

The best Box-Behnken design parameters of iron oxide removal from feldspar using Carpc magnetic separator are: magnetic field intensity 0.95 tesla, roll speed 120 rpm and feed rate 500 g/min. With these optimum parameters a non-magnetic feldspar product containing 0.249% Fe_2O_3 was obtained with 82.7% Fe_2O_3 removal and 97.5% weight of the feldspar in the non-magnetic fraction, Fig. 10.

3.5. Acid leaching process

In the process of acid leaching, the mineral comes into contact with an appropriate solvent, leading to the dissolution of minerals containing specific compounds and the generation of a concentrated solution. It is crucial to use a solvent that does not significantly affect other constituents of feldspar, preventing a deficiency of non-target elements in the final product. Therefore, organic acids could be used to dissolve iron impurities.

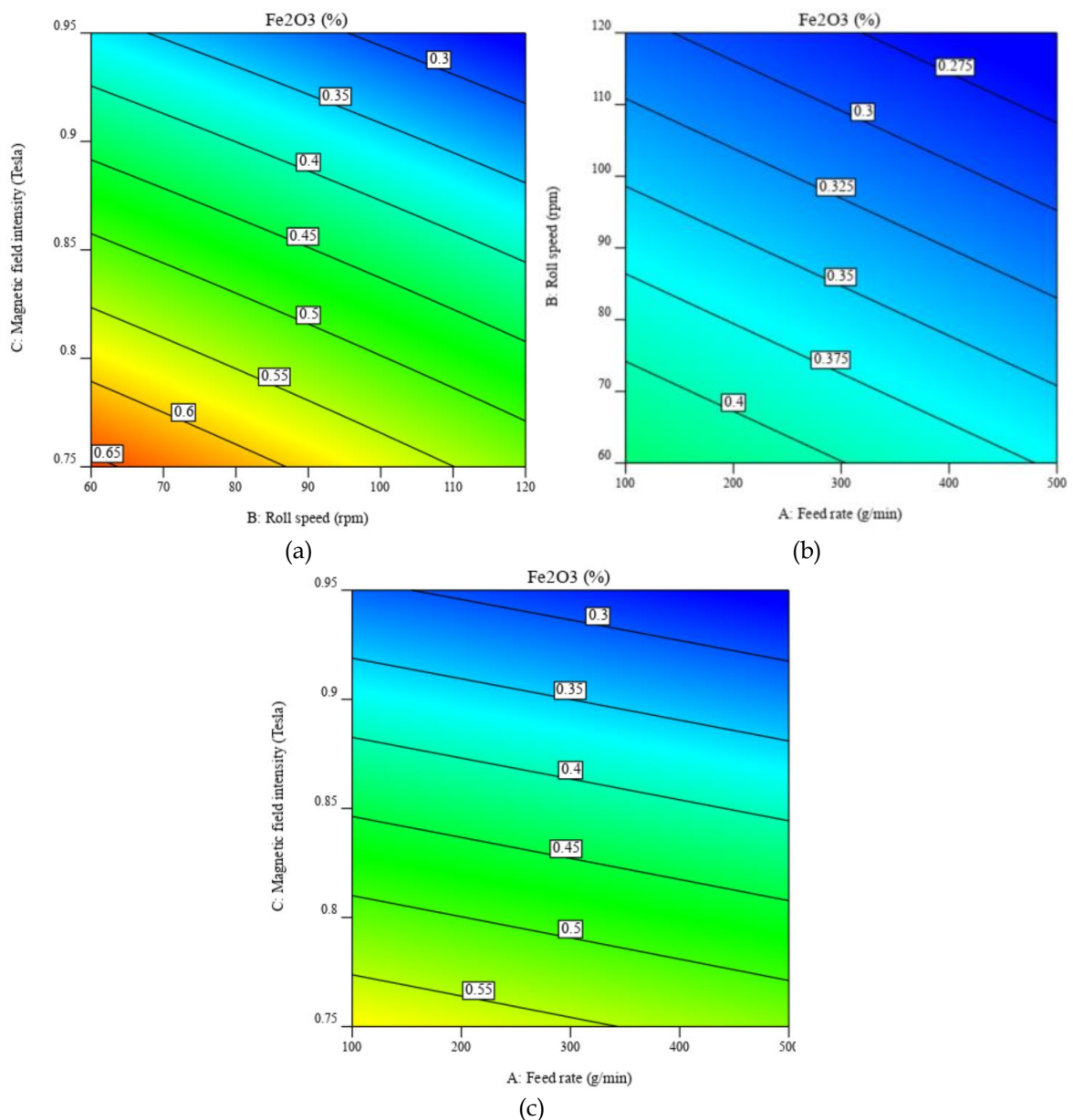


Fig. 8. The response surface plots a, b and c of iron oxide % resulting from the main effects of Carpc magnetic separator variables, magnetic field intensity, roll speed and feed rate

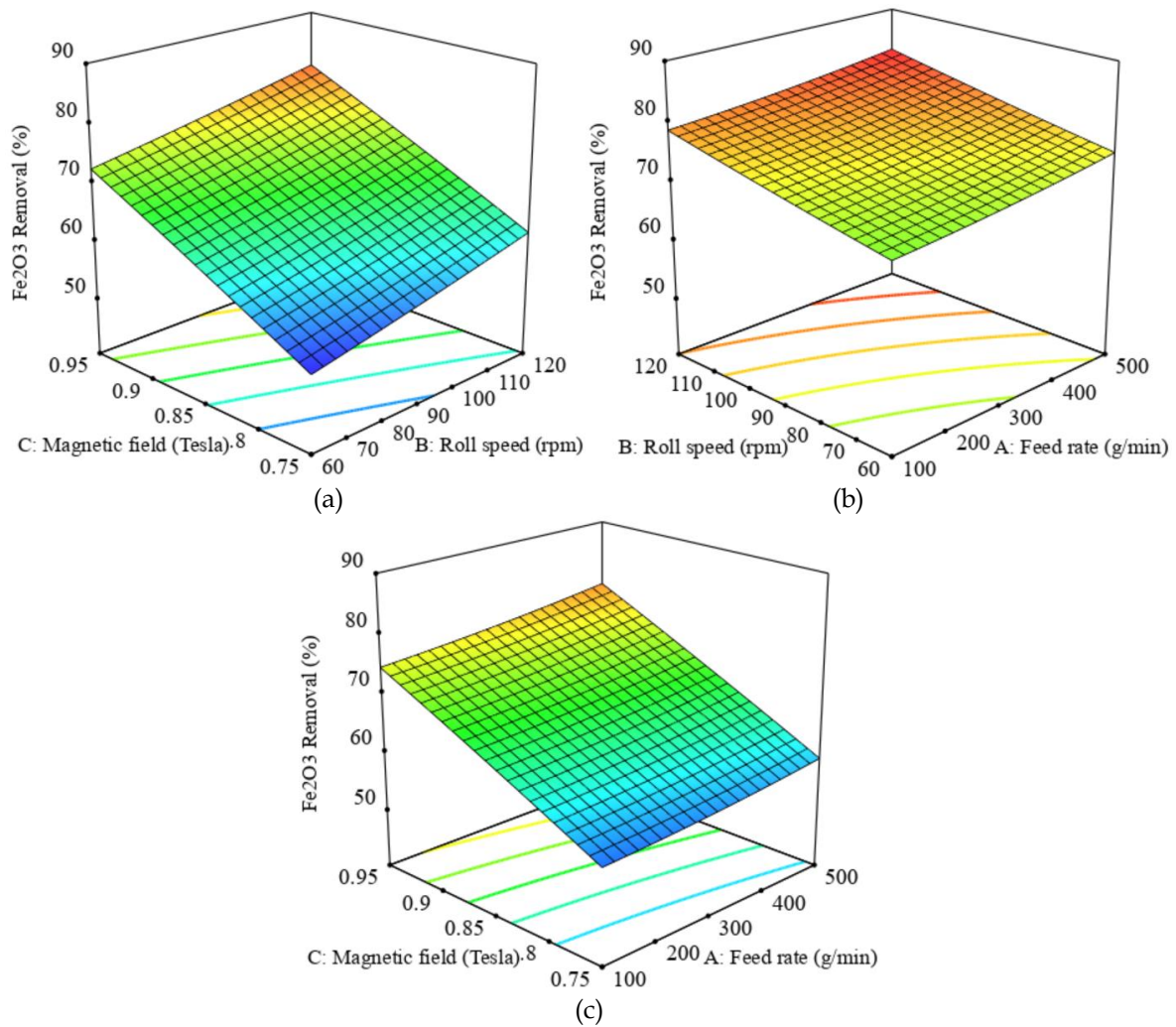


Fig. 9. The response surface plots a, b and c of iron oxide removal % resulting from the main effects of Carpc magnetic separator variables, magnetic field intensity, roll speed and feed rate

In a trial for enhancing iron oxide removal and improving feldspar whiteness, the non-magnetic feldspar concentrate was leached using oxalic and citric acids to dissolve iron oxide at different acid dosages. Leaching tests were conducted at 90°C with 60 min. as optimized previously by Abdel-Khalek et al., (2019) and the leaching process was carried out at a S/L ratio of 5% with continuous stirring speed of 1000 rpm as optimized by Pariyan et al. (2020).

Figs 11,12 displayed that increasing both oxalic and citric acid dosages up to 2 kg/ton of the non-magnetic feldspar fraction, the iron oxide decreases from 0.24% to 0.19%, and 0.22%, respectively, i.e., oxalic acid is showed slightly higher effectiveness for iron oxide removal. A higher acid dosage than 2 kg/ton has no great effect on iron oxide removal. Also, the leaching of non-magnetic feldspar fraction with oxalic acid improved the whiteness up to 85%, Table 6.

3.6. Characterization of the feldspar products

Fig. 13 shows the XRD of the final leached feldspar concentrate. It is displayed that the hematite band disappeared in the final concentrate compared to the original feldspar sample in Fig. 1. Also, the chemical analysis of the produced feldspar concentrates shown in table 5 showed the efficient removal of iron oxide from the feldspar sample. Table 6. shows the optical properties of the final product after magnetic separation and leaching by oxalic acid, which indicated increasing whiteness, brightness, and iso-brightness degrees simultaneously, decreasing redness and yellowness degrees compared to the original sample. The reduction in the contents of coloring impurities, iron oxide, reflected positively on improving the degrees of whiteness and brightness of the feldspar products.

The magnetic susceptibility values of original and treated feldspar samples are presented in Table 7. It is displayed that feldspar magnetic susceptibility is directly proportional to its iron content (Heinrich et al., 2017). Therefore, The magnetic susceptibility is highly decreased with the efficient removal of iron oxides from feldspar using successive magnetic separation and acid leaching techniques.

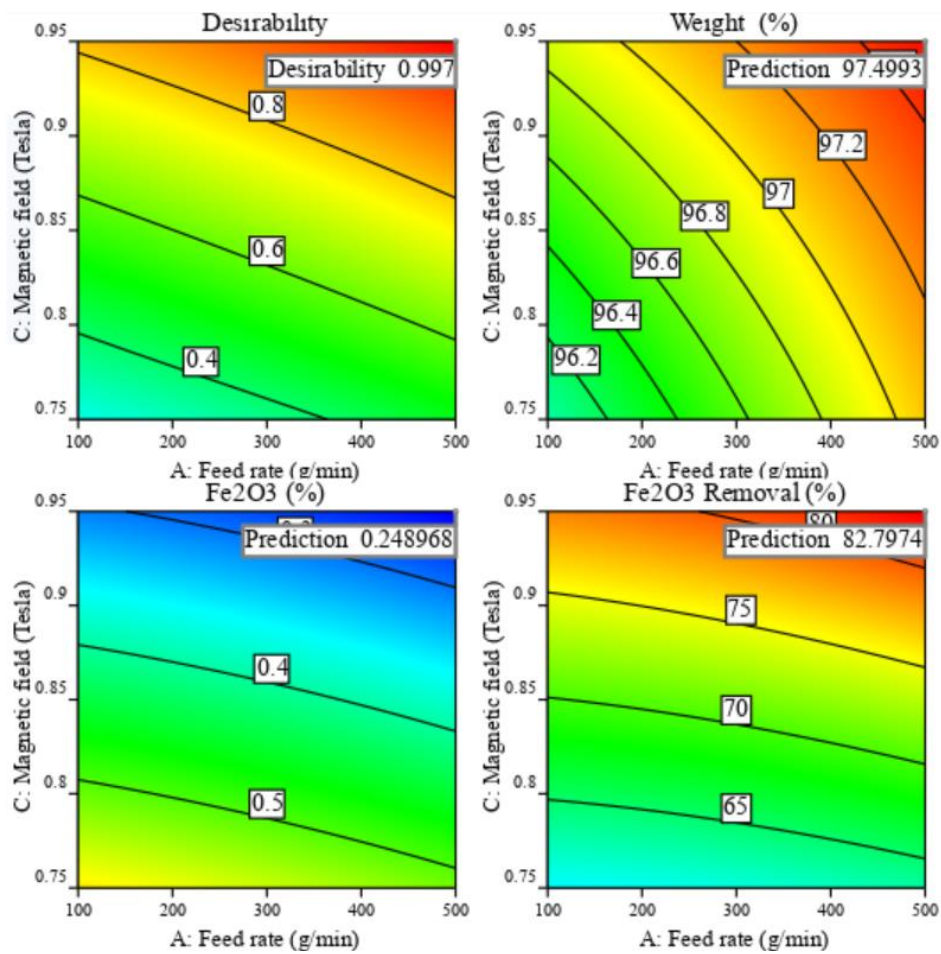


Fig. 10. CarpcO Optimization of; Desirability, % wt. of non-magnetic feldspar %, Fe₂O₃ assay % and Fe₂O₃ removal %

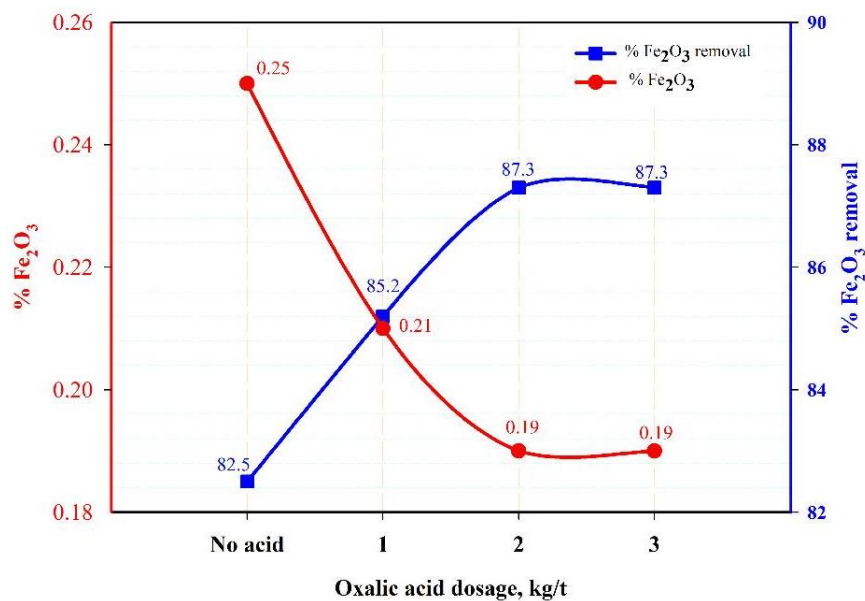


Fig. 11. Effect of oxalic acid dosage on %iron oxide and its % removal

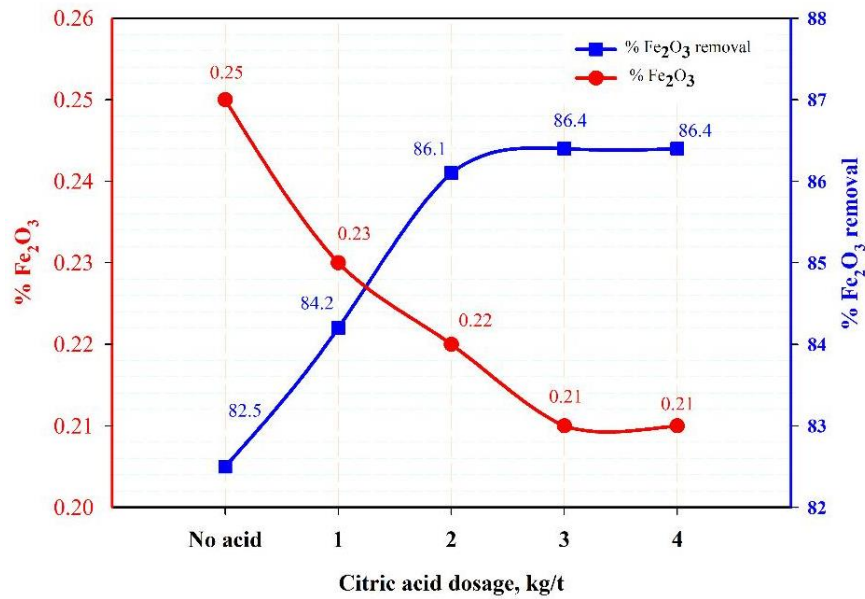


Fig. 12. Effect of citric acid on % iron oxide and iron oxide removal%

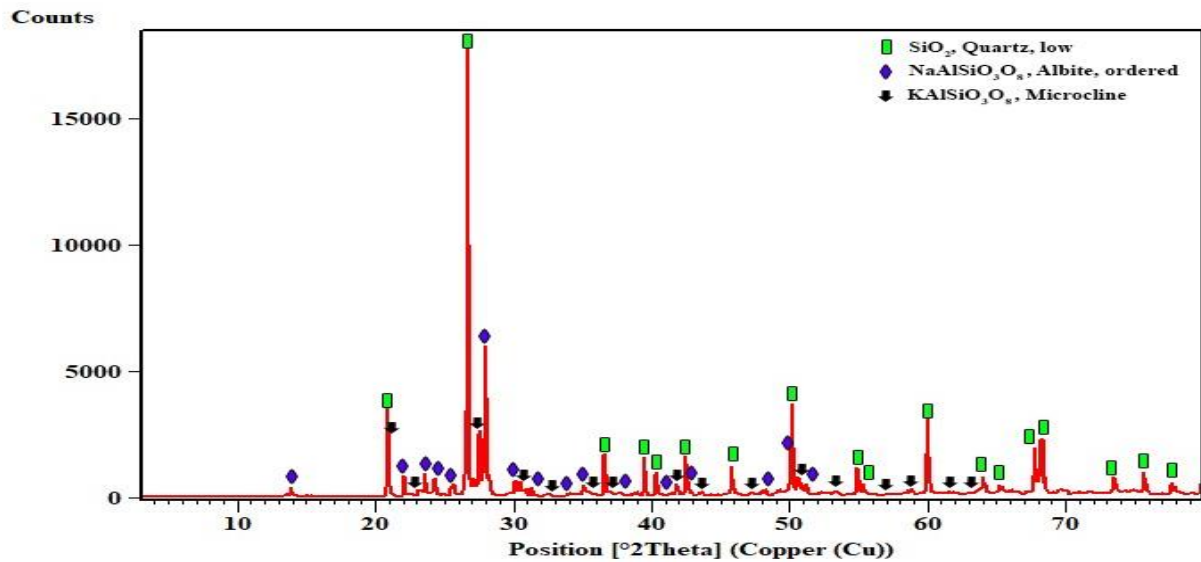


Fig. 13. XRD of the final concentrate after leaching with oxalic acid

Table 5. XRF of feldspar concentrates

Product type	SiO ₂	Al ₂ O ₃	Na ₂ O	K ₂ O	Fe ₂ O ₃	TiO ₂	CaO	MgO	Cl	L.O.I
	%									
Feldspar ore	75.870	12.480	3.220	5.360	1.400	0.091	0.930	0.074	0.040	0.533
Non-magnetic fr.	76.810	12.490	3.700	5.410	0.250	0.040	0.850	0.058	0.020	0.370
Leached feldspar	76.800	12.380	3.600	5.310	0.190	0.010	0.820	0.078	0.070	0.740

Table 6. the optical properties of the final product

property	Brightness, %	Iso-brightness, %	Whiteness, %	Redness, %	Yellowness, %
Original feldspar	30.04	42.48	65.17	12.71	42.48
Final feldspar	59.59	71.65	85.60	2.45	5.88

Table 7. Magnetic Susceptibility of original and treated feldspar

Feldspar fractions (this study)	Magnetic Susceptibility
Feldspar ore sample	$1.30 * 10^{-6}$
Non-magnetic feldspar concentrate	$1.88 * 10^{-7}$
Magnetic fraction	$1.31 * 10^{-3}$
Leached feldspar concentrate	$1.40 * 10^{-7}$
Various minerals (in Literature, Heinrich et al., 2017)	
Albite	-1.0 to -3.0 $*10^{-8}$
Quartz	-13 to -16.4 $*10^{-6}$
Biotite	$1.10 * 10^{-3}$
Chlorite	$4.90 * 10^{-4}$
Hematite	$0.50-40.0 * 10^{-3}$

4. Conclusions

This study aimed at upgrading of Wadi Zerabi feldspar ore via removing iron oxide contamination to be suitable for industrial applications. Feldspar grinding using ball mill was carried out in fractions of sizes over 250 μ m at 65% solid content in slurry, 5% powder filling, and 25% ball filling of size 36.6 mm. The desired size for Carpc magnetic separation (-250+45 μ m) is significantly increased by increasing the grinding time. Further grinding beyond 15 minutes resulted in a reduction in feed size for the magnetic separation process (-250+45 μ m) while maximizing slimes (-45 μ m).

The removal of iron oxide from feldspar ore using Carpc magnetic separator parameters was optimized via Box-Behnken design. The best design parameters are magnetic field intensity 0.95 tesla, roll speed 120 rpm and feed rate 500 g/min. With these optimum parameters a non-magnetic feldspar fraction containing 0.249% Fe₂O₃ was obtained with 82.7% Fe₂O₃ removal and 97.5% weight of the feldspar in the non-magnetic fraction.

A study on leaching of the non-magnetic feldspar was introduced using both oxalic and citric acid with optimum dosages of 2 kg/ton. The iron oxide was decreased from 0.24% to 0.19%, 0.22% respectively, i.e., oxalic acid is more effective for iron oxide removal.

The reduction in the contents of coloring impurities, iron oxide, reflected positively on improving the degrees of whiteness and brightness of the feldspar products. Therefore, the feldspar whiteness was improved from 65.17 % in the original ore to 85.60 % in the leached product.

The procedure obeyed in this study could be applied on an industrial scale. Both non-magnetic and leached feldspar products are supposed to meet the demands of ceramic and glass industries as the contents of coloring impurities including iron and titanium oxides is as less as 0.25%.

However, the silica content existed in feldspar products is considered as a drawback; therefore, a study on the removal of silica from feldspar products using flotation technique would be investigated in a future work.

Acknowledgments

The authors would like to thank the Science, Technology & Innovation Funding Authority (STDF), Ministry of Higher Education and Scientific Research, Egypt, for supporting this research work under grant number 45915.

References

ABOUZEID, A.M., NEGM, M.A., 2014. *Characterization and Beneficiation of an Egyptian Nepheline Syenite Ore*. International Journal of Mineralogy. 2014, 1-9. DOI: 10.1155/2014/128246.

- AHMED, M.M., IBRAHIM, G.A., RIZK, A.M.E., MAHMOUD, N.A., 2016. *Reduce the iron content in Egyptian feldspar ore of Wadi Zirib for industrial applications*. International Journal of Mining Engineering and Mineral Processing. 5, 25-34.
- AMAREIH, M., AL-JARADIN, M., 2014. *Characterization of the Jordanian Feldspar Raw Materials for Application in the Ceramic and Glass Industries*. International Journal of Mining Engineering and Mineral Processing. 3(2), 28-31.
- ARSLAN, V., BAYAT, O., 2009. *Removal of Fe from kaolin by chemical leaching and bioleaching*. Clays and Clay Minerals. 57(6), 787-794. doi:10.1346/CCMN.2009.057 06011.
- CAMESELLE, C., RICART, M.T., NUNEZ, M.J., LEMA, J.M. 2003. *Iron removal from kaolin. Comparison between "in situ" & "two-stage" bioleaching processes*. Hydrometallurgy. 68, 97-105.
- CINAR, M., DURGUT, E., 2019. *Mineral beneficiation of nepheline syenite with combination of dry magnetic separation and flotation methods*. Physicochemical Problems of Mineral Processing. 55(5), 1227-1238.
- DEL DACERA, D.M., BABEL, S., 2006. *Use of Citric Acid for Heavy Metals Extraction from Contaminated Sewage Sludge for Land Application*. Water Sci Technol. 54 (9), 129-35.
- DOGU, A.I., 2004. *Separation of dark-colored minerals from feldspar by selective flocculation using starch panel I*. Powder Technology. 139(3) , 258.
- ELBENDARI, A.M., ALEKSANDROV, A., NIKOLAEVA, N., AFANASOVA, A., 2020. *Selective flotation of phosphorus-bearing ores*. In E3S Web of Conferences, EDP Sciences. 192, 02021.
- ELMAHDY, A.M., MIKI, H., SASAKI, K.; FARAHAT, M., 2023. *The effect of microwave pre-treatment on the magnetic properties of enargite and tennantite and their separation from chalcopyrite*. Minerals. 2023, 13, 334. <https://doi.org/10.3390/min13030334>.
- EL-MOFTY, S.E., ELBENDARI, A.M., ABUHASEL, K.A., EL-MIDANY, A.A., 2020. *Ultrafine dry grinding of talc by planetary mill: Effects of operating conditions*. Obogashchenie Rud. 6, 21-25.
- EL-REHIEM, F.H., ABDEL-RAHMAN, M.K., 2008. *Removal of coloring materials from Egyptian albite ore*. Mineral Processing and Extractive Metallurgy. 117(3), 171-174.
- GOUGAZEH, M., 2006. *Evaluation and Beneficiation of Feldspar from Arkosic Sandstone in South Jordan for Application in the Ceramic Industry*. American Journal of Applied Sciences. 3(1), 1655-166.
- GOUGAZEH, M., 2022. *Beneficiation and upgrading of low-grade feldspar ore in Medina, Saudi Arabia*. Journal of Ecological Engineering, 23(6). DOI 10.12911/22998993/147834.
- GÜLSOY, Ö.Y., CAN, N.M., BAYRAKTAR, I., 2005. *Production of potassium feldspar concentrate from a low-grade pegmatitic ore in Turkey*. Mineral Processing and Extractive Metallurgy. 114(2), 80-86.
- GÜLSOY, Ö.Y., ORHAN, E.C., 2004. *Importance of magnet-steel configuration in dry high intensity permanent magnetic rolls: Theoretical and practical approach*. Physicochemical Problems of Mineral Processing. 38, 301-309.
- HASSAN, El-Sayed R.E., MUTELET, F., ABDEL-KHALEK, N.A., YOUSSEF, M.A., ABDALLAH, M.M., ELMENSHAWY, A.H., 2020. *Beneficiation and Separation of Egyptian Tantalite Ore*. Key Engineering Materials. 835, 208-213.
- HEINRICH, F.C., SCHMIDT, V., SCHRAMM, M., MERTINEIT, M., 2017. *Magnetic and mineralogical properties of salt rocks from the Zechstein of the Northern German Basin*. Geophys. J. Int. 208, 1811-1831.
- IBRAHIM, S.S., MOHAMED, H.A., BOULOS, T.R., 2002. *Dry magnetic separation of nepheli-nesyenite*. Physicochem. Probl. Miner. Process. 36, 173-183.
- IVETA, S., IGOR, S., PAVOL, M., MICHAL, L., 2005. *Biological, chemical and electromagnetic treatment of three types of feldspar raw materials*. Minerals Engineering. 19(4), 348.
- JENA, S. K., DHAWANA, N., RAOAD, S., MISRA, P. K., MISHARA, B. K., DAS, B., 2014. *Studies on Extraction of Potassium Values from Nepheline Syenite*. International Journal of Mineral Processing. 133, 13-22.
- JONGLERTJUNYA, W., RUBCUMINTARA, T., 2013. *Titanium and Iron Dissolutions from Ilmenite by Acid Leaching and Microbiological Oxidation Techniques*. Asia Pacific Journal of Chemical Engineering. 8 (3), 323-330.
- KAR, B., SAHOO, H., RATH, S.S., RAO, D.S., DAS, B., 2013. *Characterization and beneficiation studies for the removal of iron from a china clay from India*. Clay Minerals. 48(5), 759-769. doi:10.1180/claymin.2013.048.5.08.
- LIU, Y., PENG, H., HU, M., 2013. *Removing iron by magnetic separation from a potash feldspar ore*. Journal of Wuhan University of Technology-Mater. Sci. Ed. 28(2), 362-366.
- MAGDALINOYIC, N. TRUMIC, M. ANDRIC, L., 2012. *The optimal ball diameter in a mill*. Physicochem. Probl. Miner. Process. 48(2), 329-339.
- PANE, I.V., FUERTES, J.J., REINOSA, J.F., FERNANDEZ, E., ENRIQUE, Z., 2022. *Engineered feldspar-based ceramics: A review of their potential in ceramic industry*, Journal of the European Ceramic Society. 42(2), 307-326.

- PARIYAN, K., HOSSEINI, M.R., AHMADI, A., ZAHIRI, A., 2020. *Optimization and kinetics of oxalic acid treatment of feldspar for removing the iron oxide impurities*. Separation Science and Technology. 55, 1871-1882. DOI: 10.1080/01496395.2019.1612913.
- ROSTOM, M., HASSAN, EL-Sayed R.E., GABER, M.S., EL ENSHASY, H., 2020. *Treatment of Egyptian wastepaper using flotation technique for recovery of fillers and minerals*. International Journal of Scientific & Technology Research. 9, 3077-3083.
- SAISINCHAI, S., BOONPRAMOTE, T., MEECHUMNA, P., 2015. *Upgrading feldspar by WHIMS and flotation techniques*. Engineering Journal. 19(4), 83-92.
- SILVA, J.C., ULSEN, C., BERGERMAN, M.G., HORTA, D.G., 2019. *Reduction of Fe₂O₃ content of foyaite by flotation and magnetic separation for ceramics production*. Journal of Materials Research and Technology. 8, 4915-4923.
- ŠTYRIAKOVÁ, I., ŠTYRIAK, I., GALKO, I., HRADIL, D., BEZDIČKA, P., 2003. *The release of iron-bearing minerals and dissolution of feldspars by heterotrophic bacteria of Bacillus species*. Ceramics-Silikáty 47(1), 20-26.
- VAPUR, H., TOP, S., DEMIRCI, S., 2017. *Purification of feldspar from colored impurities using organic acids*, Physicochemical Problems in Mineral Processing. 53, 150-160.
- XU, J., CHEN, J., REN, X., XIONG, T., LIU, K., SONG, S., 2022. *A novel dry vibrating HGMS separator for purification of potash feldspar ore*. Separation Science and Technology. 57(3), 484-491.
- ZHANG, Y., HU, Y., SUN, N., LIU, R., WANG, Z., WANG, L., SUN, W., 2018. *Systematic review of feldspar beneficiation and its comprehensive application*. Minerals Engineering. 128, 141-152.
- ZHAO, R C., HAN, Y. X., HE, M.Z., LI, Y.J., 2017. *Grinding kinetics of quartz and chlorite in wet ball milling*. Powder Technol. 305, 418-425.